ACS APPLIED MATERIALS & INTERFACES

Research Article

www.acsami.org

Improved Electrical Performance and Bias Stability of Solution-Processed Active Bilayer Structure of Indium Zinc Oxide based TFT

Jin-Suk Seo and Byeong-Soo Bae*

Laboratory of Optical Materials and Coating (LOMC), Deptartment of Materials Science and Engineering, Korea Advanced Institute of Science and Technology (KAIST), Daejeon 305-701, Republic of Korea

Supporting Information

ABSTRACT: We fabricated active single- and bilayer structure thin film transistors (TFTs) with aluminum or gallium doped (IZO:Al or IZO:Ga) and undoped indium zinc oxide (IZO) thin film layers using an aqueous solution process. The electrical performance and bias stability of these active single- and bilayer structure TFTs were investigated and compared to reveal the effects of Al/Gal doping and bilayer structure. The single-layer structure IZO TFT shows a high mobility of 19 $cm^2/V{\cdot}s$ with a poor positive bias stability (PBS) of ΔV_T + 3.4 V. However, Al/Ga doped in IZO TFT reduced mobility to 8.5−9.9 $cm^2/V{\cdot}s$ but improved PBS to ΔV_T + 1.6−1.7 V due to the reduction of oxygen vacancy. Thus, it is found the bilayer structure TFTs with a combination of bottom- and top-layer compositions modify both the mobility and bias stability of the TFTs to be optimized. The bilayer structure TFT with an IZO:X bottom layer possess high mobility and an IZO bottom layer improves the PBS.

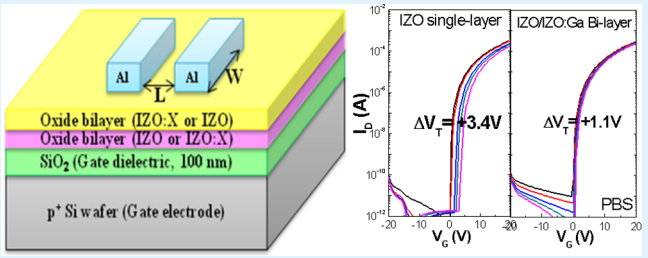

KEYWORDS: *metal oxide TFT, indium zinc oxide, solution process, active bilayer structure, field effect mobility, bias stability*

1. INTRODUCTION

Amorphous metal oxide semiconductors (AOSs) have been extensively studied as the active layers in display backplanes of thin film transistors (TFTs) that have many advantages such as high mobility and optical transparency, and the amorphous state is attractive for large-area uniformity.[1−3] Most of all, both the amorphous state and high mobility are very attractive to alternative active materials instead of conventional a-Si:H (<1 $cm^2/V{\cdot}s$) from the perspective of fabrication and applications.[4] The conventional a-Si:H TFT has already limits to fulfill the high-end specifications as display backplane due to its low mobility: UD (ultradefinition high resolution), 480 Hz (high frame rate), and large size (>50 in., RC delay).[4,5] Also, poly-Si TFTs have critical problems in mass-production since they take a long time to make their crystalline structure with large-area uniformity.[4] From now, new AOS materials are being developed by many researchers based on zinc-oxide materials such as zinc oxide (ZO), indium oxide (IO), indium zinc oxide (IZO), zinc tin oxide (ZTO), and indium gallium zinc oxide (IGZO) composition and surveyed stabilizer ions (Hf, Zr, Li, Mg, Al ets) in an oxide system.[4−12] The most well-known representative of AOS materials, amorphous indium−gallium−zinc-oxide (a-IGZO) was first reported by Hosono et al.[1] Either in a vacuum process or solution process, the multicomponent materials are more attractive than intrinsic or binary compositions because these materials make a stable amorphous oxide structure and facilitate control of the carrrier density.[5,13,14] And most of the stabilizer ions act as a carrier surppressor and reduce oxygen deficiencies.[1,2,6−12,14−19] For the stabilizer ions, two representative precursors of aluminum and gallium atoms were doped to tune the electrical mobility and the bias stability, especially in oxide TFT fabricated by the solution process.[19]

Nowadays, the sol−gel method is an attractive process to replace the conventional vacuum process due to its ease of fabrication, scalability, and lower cost.[3] One of the key parameters in the solution process is the solvent, which determines the properties of coated wet films, the solution mechanism, and a conservative property of precursor solution, among other properties.[3] Impurity-free water is a good solvent because it has no volatile organic compounds or organic residues to be removed to create high-performance oxide TFTs.[16,17] Thus, the aqueous precursor solutions can make the pure metal oxide without high-temperature annealing, and they show good electrical stability.[16,17] The fabricated aqueous fluorine-doped indium zinc oxide (IZO:F) TFTs on a flexible substrate showed a high field-effect mobility of 4.1 $cm^2/V{\cdot}s$ at low-temperature annealing at 200 °C and good stabilities in previous reports.[17] In terms of fabrication process, IGZO thin-films was easily damaged due to its poor chemical stability if the back-channel-etch (BCE) structure was employed, so it is essential to adopt the etch stopper-layer (ESL) structure.[20] Thus, the combination of the optimized oxide composition and TFT design is important to show both good electrical

Received: June 17, 2014
Accepted: August 12, 2014
Published: August 12, 2014

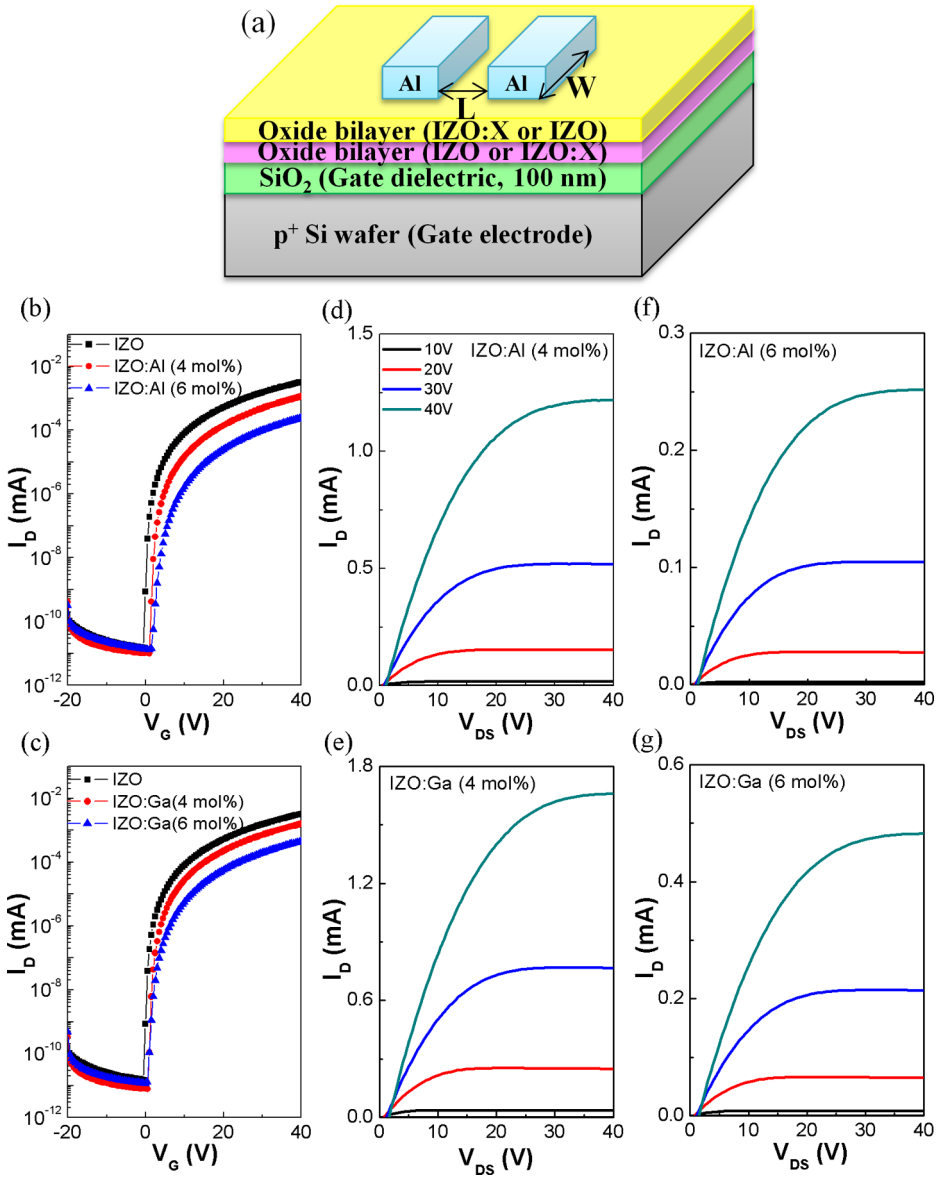

Figure 1. (a) Structure image of oxide TFT and evolution of the transfer (b and c) and output curves (d–g) of active single-layer IZO:Al and IZO:Ga TFTs, respectively, as a function of the Al and Ga doping concentration (4 and 6 mol %) (V_{DS} = 40 V, V_G = −20–+40 V).

performance and stability. Recently, active bilayer structure was studied since it was expected to achieve both high mobility and good bias stability by combining two different composition semiconducting thin film channel layers.[21] To protect the active bottom layer of IZO or IGZO, chemical durable ZTO and Cu-doped IGZO materials were adapted as an active top layer in BCE structure and the IGZO/ZTO[20] and IGZO/Cu-GIZO[22] bilayer structure show superior TFT performance and stability. Also, IO/IGO,[21] IZO/IGZO,[23] IO/GO,[24] IZO or ITO/GIZO,[25] IGZO/IGZO:Ti,[26] IZO/ZTO,[27] AZO/ZO,[28] and HZO/ZO/HZO[29] multilayer structure TFTs demonstrate significantly enhanced performance and/or bias stability using either vacuum or solution process. Using an active single-source, different Hf contents[8] or varying the O_2/Ar gas ratio[30,31] was adopted as active bilayer composition, which performed as well as highly stable TFTs.

In this paper, the aluminum and gallium were doped into active IZO thin films fabricated by a metal-fluoride-precursor-based aqueous solution process to improve the gate bias stability of the TFT. Then, the active bilayer structure TFTs composed of Al- and Ga-doped IZO (IZO:X, X = Al, Ga) and undoped IZO thin films were fabricated and studied to achieve both high mobility and good bias stability.

2. EXPERIMENTAL SECTION

A 0.15 M IZO precursor solution was prepared by directly dissolving indium fluoride trihydrate ($InF_3{\cdot}3H_2O$ > 99%) and zinc fluoride (ZnF_2, 99%) in water (H_2O, ACS reagent) at room temperature. The optimized molar ratio of In: Zn was 1:2 in IZO solution and 2:1 in IZO:Al and IZO:Ga precursor solutions. The sources for aluminum and gallium were aluminum nitrate nonahydrate [$Al(NO_3)_3{\cdot}9H_2O$ > 99.99%] and gallium nitrate hydrate [$Ga(NO_3)_3{\cdot}xH_2O$ > 99.99%], respectively. All reagents were purchased from Sigma-Aldrich and were used without further purification. The aqueous solution was stirred for 4 h and filtered through a 0.22 μm syringe filter. The thermal behavior of the precursor was investigated by using a thermogravimetric analyzer (TA Instrument). The precursor solution was dried at 100 °C to remove the water solvent, and the powder was analyzed. The temperature ramping rate was 5 °C/min, and the analyzer was heated up to 800 °C.

Table 1. Electrical Properties of Optimized Composition TFT with Active Single-Layer and Bilayer Thin Films Annealed at 350°C

active layer	metal oxide (bottom/top)	I_{on}/I_{off}	μ (cm^2/ V·s)	V_T (V)	S.S. (V/dec)	NBS (ΔV_T)	PBS (ΔV_T)
single layer	IZO	2.1×10^8	19.0 ± 1.9	8.5 ± 1.3	0.28 ± 0.04	−0.1 ± 0.2	+3.4 ± 1.6
	IZO:Al (4 mol %)	1.1×10^8	8.5 ± 1.1	11.9 ± 0.2	0.31 ± 0.23	−1.4 ± 0.8	+1.7 ± 0.7
	IZO:Ga (4 mol %)	2.0×10^8	9.9 ± 1.4	9.8 ± 0.5	0.29 ± 0.14	−1.0 ± 0.4	+1.6 ± 0.6
	IZO:Al (6 mol %)	1.7×10^7	2.0 ± 0.6	13.2 ± 0.6	0.62 ± 0.14		
	IZO:Ga (6 mol %)	3.4×10^7	3.2 ± 0.7	11.5 ± 0.2	0.54 ± 0.07		
bilayer	IZO/IZO	2.2×10^8	17.3 ± 1.3	11.4 ± 0.3	0.41 ± 0.12		
	IZO:Al (4 mol %)/IZO	5.5×10^7	23.4 ± 0.7	9.3 ± 0.7	0.27 ± 0.13	−0.53 ± 0.82	+2.1 ± 0.7
	IZO/IZO:Al (4 mol %)	6.9×10^7	8.8 ± 1.8	10.8 ± 1.1	0.68 ± 0.08	−0.32 ± 0.41	+1.3 ± 0.4
	IZO:Ga (4 mol %)/IZO	2.7×10^8	19.4 ± 2.3	7.7 ± 1.2	0.20 ± 0.24	−0.32 ± 0.28	+2.3 ± 0.8
	IZO/IZO:Ga (4 mol %)	1.3×10^8	13.7 ± 1.7	9.1 ± 0.9	0.27 ± 0.14	−0.20 ± 0.17	+1.1 ± 0.4

To fabricate the device, a 100 nm SiO_2 was thermally grown as a gate dielectric layer on the top of a heavily boron(p^+)-doped Si wafer. In the case of single-layer structure TFTs, the synthesized precursor solutions were spin-coated at 5000 rpm for 30 s on substrates that were treated by oxygen plasma, and the coated active layer was annealed on a hotplate at 350 °C for 2 h under ambient atmosphere. In the case of bilayer structures, each active layer in the bilayer structure was annealed for 1 h under the same spin-coating conditions and the bottom layer was annealed for a total of 2 h. The top-layer precursor solution was immediately spin-coated onto the fabricated bottom-layer to avoid environmental contamination after cooling the bottom layer. The Al source and drain electrodes were deposited by an e-beam evaporator (pressure ~10^{-6} Torr) through a shadow mask that has a channel length and width of 100 and 1000 μm, respectively. We have fabricated at least 10 devices for each TFT structure, and we have calculated the average TFT characteristics of these separately fabricated single- and bilayer TFTs.

The chemical composition of oxide films was examined by X-ray photoelectron spectroscopy (XPS, Sigma Probe, Thermo VG Scientific). The data were collected using monochromatic Al K radiation (1486.6 eV) in an ultrahigh vacuum system with a base pressure of ~10^{-10} Torr. The surface morphology and roughness of the oxide thin films were characterized by atomic force microscopy (AFM, Park system XE-100) with noncontact mode. High-resolution cross-sectional transmission electron microscopy images and selected-area diffraction patterns (HR-TEM, FEI, Tecnai TF30 ST) were obtained with an electron acceleration voltage of 300 kV. The TEM samples were prepared using focused ion beam (FIB, Quanta 3D FEG) techniques. Electrical characterization and stability were performed using the semiconductor parameter analyzer 4156A. The gate bias stress of ±20 V was applied with V_{DS} = 0 V at N_2 inert conditions. For the data reliability, we have measured the TFT stability of at least three devices for each TFT structure that has the average TFT performance.

3. RESULTS AND DISCUSSION

Metal fluoride precursors are hydrolyzed into indium hydroxide and zinc hydroxyl fluoride at room temperature, and the indium and zinc hydroxide forms are condensed into indium and zinc oxide over 250 and 380 °C, respectively.[17] From the TGA data (as shown in Figure S1, Supporting Information), aluminum and gallium nitrate precursors are hydrolyzed into aluminum and gallium hydroxide, and thermally oxidized into aluminum and gallium oxide around 250 and 200 °C, respectively.[32] Thus, aluminum and gallium oxides are generated at much lower temperatures than zinc oxide, and the aluminum and gallium atoms are known to be more effective suppressors than those of the zinc precursor because their high ionic potential (+ 3 valence and small ionic radius) forms stable oxide structure and controls the oxygen vacancy and carrier concentration.[2] The ionic potential gives a sense of how strongly the ion will be attracted to ions of opposite charge or repelled to other ions of like charge.[33] In the literature, ionic potential values of Al^{3+}, Ga^{3+}, In^{3+}, and Zn^{2+} are 119.99, 64.0, 54.0, and 39.7 eV, respectively.[34] Thus, it is expected the doping effect will be clearly shown, even though a small amount of aluminum and gallium is doped in IZO TFTs.

Figure 1 shows the evolution of transfer and output curves of single-layer structure TFT as a function of Al and Ga doping concentration. The on-current is largely decreased with increasing Al and Ga doping contents in the IZO thin films, but the off-current remains lower than 10^{-11}A. Thus, the density of free carriers that are sensitive to the on-current is effectively suppressed by the doped Al and Ga atoms. The reduced density of free carriers directly influences field-effect mobility, which is dramatically decreased. Table 1 summarizes the electrical properties of various TFTs annealed at 350 °C for 2 h. The undoped single-layer IZO TFT shows high-performance transistor characteristics, with a mobility of 19.0 cm^2/V·s and an on−off current ratio (I_{on}/I_{off}) of approximately ~10^8 measured at a drain-source voltage (V_{DS}) of 40 V and a gate voltage (V_G) swing from −20 to +40 V.[17] The output characteristics of active single-layer thin layers are saturated at various gate voltages (0−40 V) and exhibit the good n-channel property. And the output current also decreases with increasing Al and Ga doping contents in the IZO thin films, as shown in Figure 1 (d−g). When the suppressors are doped in IZO TFT, the mobility of IZO:Al (4 mol %) and IZO:Ga (4 mol %) TFT is reduced to 8.5 and 9.9 cm^2/V·s, respectively. Furthermore, the mobility of IZO:Al (6 mol %) and IZO:Ga (6 mol %) TFT further decreases to 2.0 and 3.2 cm^2/V·s, respectively. The mobility of IZO:Al TFT is slightly lower than the IZO:Ga TFT due to its higher ionic potential.[34] In order to know the Al and Ga doping effect on single-layer structure, a TFT stability test was examined according to positive and negative bias stress (PBS and NBS, respectively). A gate bias stress of V_G = ± 20 V was applied under inert dark conditions to avoid the back-channel and illumination effect. It was measured at a drain-source voltage (V_{DS}) of 20 V and a gate voltage (V_G) swing from −20 to +20 V. As shown in Figure 2, the stability curves with the reduced V_G swing and V_{DS} decrease in the on-current and mobility compare to the transfer curves of Figure 1. When NBS is applied, the ionized oxygen vacancies will be attracted toward the channel, while the channel electrons migrate toward the back-channel. Under PBS, electrons trapping at or near the active channel-insulator interface lead to the decrease in off-current and a positive V_T shift.[35] As shown in Figure 2a, the single-layer IZO TFT shows robust NBS where threshold voltage (ΔV_T) shifts −0.1 V, but PBS greatly changes the ΔV_T

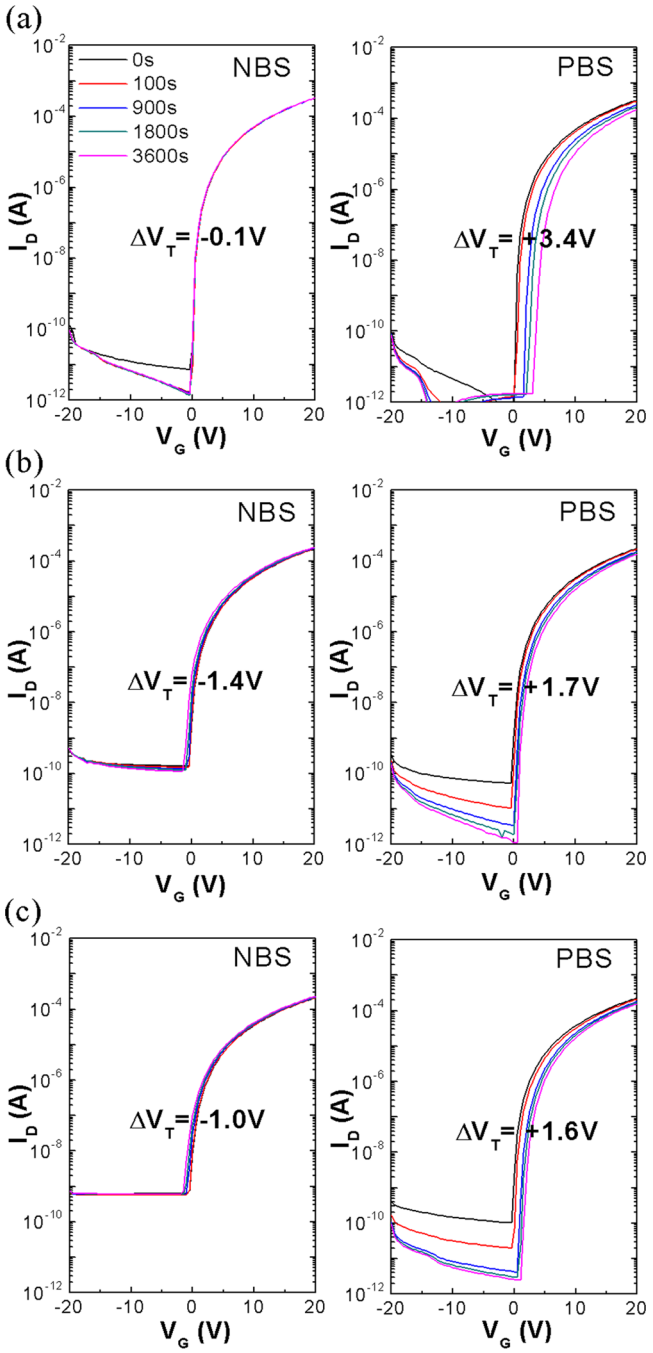

Figure 2. Negative (−20 V) and positive (+20 V) gate bias stability of active single-layer (a) IZO, (b) IZO:Al (4 mol %), and (c) IZO:Ga (4 mol %) TFTs (V_{DS} = 20 V, V_G = −20−+20 V).

of by +3.4 V. On the other hand, the single-layer IZO:Al and IZO:Ga TFTs show different behavior of bias stability, as shown in Figures 2b,c. Their threshold voltage shifts are −1.4 V, −1.0 V (NBS) and +1.7, +1.6 V (PBS), respectively. Thus, PBS of the single-layer IZO:X TFT is enhanced by the Al and Ga doping effect compared to that of the undoped IZO TFT (+3.4 V), but NBS is slightly deteriorated.

In sequence, the representative transfer curves and output curves of bilayer structure TFTs are shown in Figure 3, respectively. To compare the bilayer structure effect on the TFT performance, a translocated structure of the bottom/top layer was fabricated with both IZO/IZO:X and IZO:X/IZO TFTs (X = Al and Ga, 4 mol %). The calculated electrical properties of all the bilayer structure TFTs are summarized in Table 1. It is already reported that the electrical conductivity is determined by the bottom layer in the bilayer structure TFT, which mainly forms the current path in the channel/dielectric interfaces.[28,29] However, the bilayer structure IZO/IZO:Al (4 mol %) and IZO/IZO:Ga (4 mol %) TFTs with an undoped composition bottom layer show smaller mobilities (8.8 and 13.7 $cm^2/V{\cdot}s$, respectively) than undoped single-layer IZO TFT. On the other hand, another bilayer structure of IZO:Al/IZO and IZO:Ga/IZO TFTs with a doped composition bottom layer represents the greatly enhanced mobilities (23.4 and 19.4 $cm^2/V{\cdot}s$, respectively) compared to the doped single-layer IZO:X TFT. Thus, the mobility of the bilayer structure TFT follows that of top-layer composition rather than bottom-layer composition.

Also, the bias stability of bilayer structure TFTs were examined, as shown in Figure 4, and compared with that of single-layer structure TFTs. It is also known the bias stability of the bilayer structure TFT was improved due to the use of a bias stable composition top layer.[23,25,27−30] The bilayer structure IZO/IZO:Al and IZO/IZO:Ga TFTs with an undoped composition bottom layer shows the better PBS results with smaller ΔV_T (+1.3 and +1.1 V, respectively) than single-layer structure IZO, IZO:Al, and IZO:Ga (+3.4, +1.7, and +1.6 V, respectively) TFTs. Also, NBS is enhanced in the bilayer structure TFTs from −1.4 and −1.0 V (single-layer structure IZO:Al and IZO:Ga TFTs, respectively) to −0.32 and −0.2 V (bilayer structure IZO/IZO:Al and IZO/IZO:Ga TFTs, respectively), although those values are comparable to that of the single-layer structure IZO TFT (−0.1 V). Moreover, the bilayer structure IZO:Al/IZO and IZO:Ga/IZO TFTs with a doped composition bottom-layer show the better PBS results with smaller ΔV_T (+2.1 and +2.3 V, respectively) than single-layer structure IZO TFTs (+3.4 V). On the other hand, the NBS is improved from −1.4 and −1.0 V (single-layer structure IZO:Al and IZO:Ga TFTs, respectively) to −0.53 and −0.32 V (bilayer structure IZO:Al/IZO and IZO:Ga/IZO TFTs, respectively). Thus, the bilayer structure TFTs are very sensitive to the bias stability as well as the electrical properties to optimize its performance by the combination of bilayer compositions.

Influence of Al and Ga cation doping on the electrical properties and bias stability is explained by XPS composition analysis (see Figure S2, Supporting Information). The chemical composition of the single-layer thin films is summarized in Table 2, and the calculated indium and zinc ratio is 1:2.1 in undoped IZO films and 1.7−2.0:1 in IZO:X films. The composition of the IZO:X thin films is optimized with a more indium-rich ratio than the IZO thin film because the small quantity of Al and Ga atoms act as an effective suppressor. The Al and Ga concentration over metal contents is as small as 3.8−4.5 at. %. Thus, the experimental results of chemical composition coincide with theoretical data. In the XPS spectra, the oxygen 1s peak was deconvoluted into three different peaks at 530.7, 532.0, and 532.9 eV, which were assigned to oxygen in the oxide lattice without vacancy, with the oxygen vacancy and with the hydroxyl group, respectively (shown in Figure S3, Supporting Information).[17] The amount of hydroxyl group in single-layer IZO:Al and IZO:Ga thin films increases more than that of undoped IZO thin films, and the peaks of metal oxygen and oxygen vacancy slightly decrease in single-layer IZO:Al and IZO:Ga thin films. These mean the Al and Ga atoms suppress

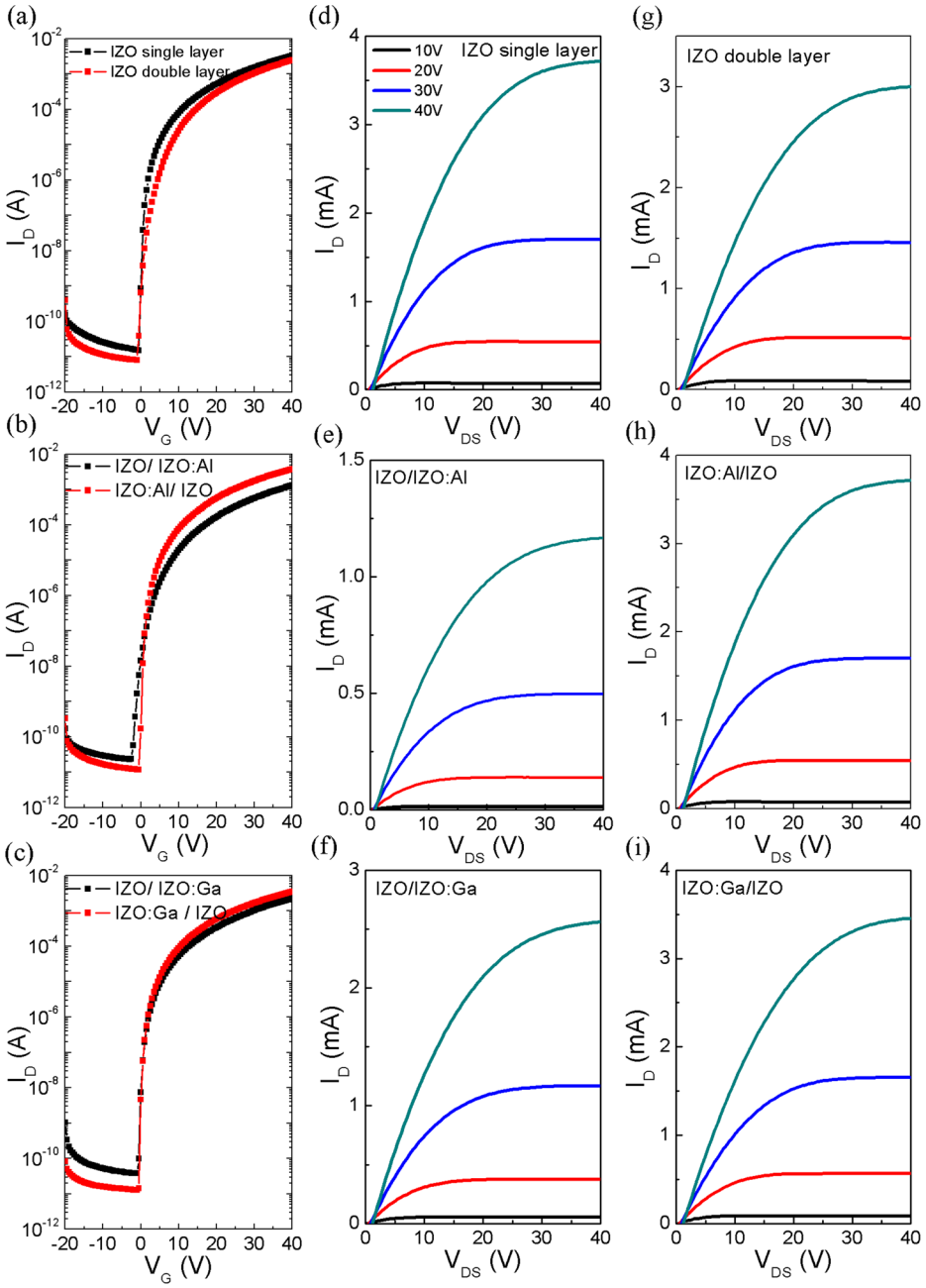

Figure 3. Representative transfer (a–c) and output curves (d–i) of active single- and double-layer IZO, bilayer IZO/IZO:X, and bilayer IZO:X/IZO TFTs (V_{DS} = 40 V, V_G = −20–+40 V).

the formation of oxygen vacancy by forming strong metal-oxide networks (M_1–O–M_2) in the IZO matrix.[14,18] That was demonstrated by Jung et al. using electron paramagnetic resonance (EPR) investigation, which revealed the decreased oxygen vacancy concentration in Ga-doped ZTO films and the reduced ΔV_T shift in PBS.[18] Likewise, the Al and Ga cations, having a high ionic potential, make a strong oxygen bond and reduce oxygen vacancies.[2] Thus, the PBS of single-layer IZO:X TFT is improved by the reduced oxygen vacancy related to electron trap sites. On the other hand, the increased hydroxyl groups (M–OH) represent one of the incomplete oxide bonds due to the remaining aluminum and gallium hydroxide groups in the IZO:X thin films.[15,18] The increased hydroxide groups in IZO:Al and IZO:Ga thin films act as hole trap sites that can deteriorate the NBS.[19] Therefore, the amount of hydroxide group is IZO:Al > IZO:Ga > IZO and the undoped single-layer IZO TFT shows the best NBS results. The V_T shift in PBS shows almost identical results in IZO:Al (+1.7 V) and IZO:Ga (+1.6 V), but the V_T shift of IZO:Ga (−1.0 V) is more resistive than that of IZO:Al (−1.4 V) in the NBS test. The hydroxide group can be reduced by an advanced annealing process such as a high pressure O_2 annealing method.[15]

To know the effect of the active bilayer structure TFT, XPS depth analysis was performed to confirm the chemical composition. In the case of bilayer structure IZO/IZO:X thin films, the bottom and top active layers used different indium and zinc ratios, and they showed a gradual change in the atomic compositions, as listed in Table 3 and represented in Figures S4,5 (Supporting Information). At 20 s of Ar^+ sputtering time, the calculated atomic ratio of indium and zinc was around 1:2,

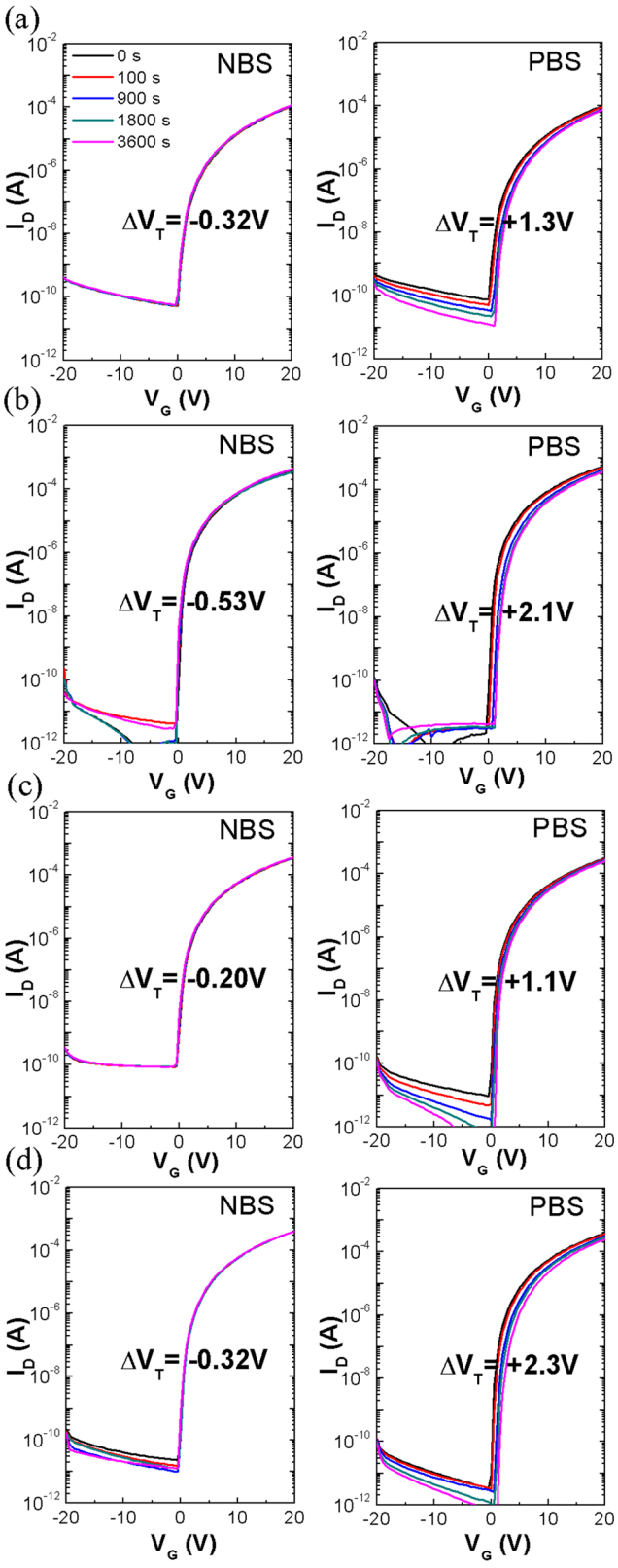

Figure 4. Negative (−20 V) and positive (+20 V) gate bias stability of active bilayer (a) IZO/IZO:Al, (b) IZO:Al/IZO, (c) IZO/IZO:Ga, and (d) IZO:Ga/IZO TFTs (V_{DS} = 20 V, V_G = −20−+20 V).

which resembles the composition of the bottom-layer IZO thin film (Ar^+ sputtering position might be slightly close to the bottom-layer thin films) and the doping concentration of X is about 3.7−4.2 at. %. In the further interior compositions, the dopants are also diffused into the bottom layer, and their concentrations are around 4.1−5.3 at. % at 40 s of Ar^+ sputtering time. At that time, the intensity of the indium and zinc peaks decreases and the oxygen peak changes due to a projected SiO_2 layer underneath. As the Ar^+ sputtering time increases, the Si 2p peak of the Si/SiO_2 substrate increases and the metal oxide peaks decrease from the upper IZO:X to the lower IZO thin films. These results indicate that the analyzed position is nearby the interface of oxide and SiO_2 gate insulator. When the upper active layer is spin-coated after annealing the lower oxide layer, the later precursor solutions might penetrate the pore and/or traps of the bottom thin film layers.[20,36] Thus, the suppressors of X in top-layer IZO:X are diffused into the bottom-layer IZO with high-temperature annealing at 350 °C.[27] The mobility of the bilayer structure IZO/IZO:X TFT decreases compared to the single-layer structure IZO TFT because the bottom-layer IZO TFT is doped by suppressors like IZO:X TFT. As previously explained, the field-effect mobility of single-layer IZO:X TFT is effectively decreased by the doped Al and Ga atoms. And the top-layer IZO:X TFT contributes to decreasing the total carrier concentration in bilayer structure IZO/IZO:X TFT.[21,23,25,26,29,31]

In the case of other bilayer structure IZO:X/IZO thin films, the calculated atomic ratio of indium and zinc is around 1:1 at 20 s of Ar^+ sputtering time, which is the averaged value of the composition of top- and bottom-layer thin films (Ar^+ sputtering position might be in the middle of active bilayer thin films) and a doping concentration of X is about 0−0.8 at. %. If the IZO:X thin films exists in the bottom layer, the suppressors of X are relatively difficult to diffuse into the top layer due to its solid state. At 40 s of Ar^+ sputtering time, the concentration of dopants is around 2.6−2.7 at. %. For these reseons, the mobility of the bilayer structure IZO:X/IZO TFT increases compared to the single-layer structure IZO:X TFT because the high mobility of top-layer IZO TFT contributes to increasing the total carrier concentration. Therefore, the total carrier concentrations in bilayer structure IZO/IZO:X and IZO:X/IZO TFTs is affected by the thermal-diffusion of the top-layer precursor. To consider the thickness effect, a double-coated IZO TFT was fabricated, and it showed similar electrical performances, with a mobility of 17.3 $cm^2/V{\cdot}s$, compared with the single-layer IZO TFT. The active thickness is an important parameter related to the carrier concentration, and the active thickness of bilayer structure TFT increases compared to that of single-layer TFT.[21,24−30] The use of active heterojunction structure IZO:X/IZO TFT shows a similar/or improved electrical mobility compared to the active homojunction structure IZO/IZO TFT with the same bilayer composition, even though they have a lower mobility of bottom-layer IZO:X.[23] Thus, the electrical properties of bilayer structure are influenced by not only the thickness of active thin films but the interfacial property. As previously mentioned in the XPS results, the IZO:X thin films have more hydroxide groups than IZO thin films, and these groups might produce better interfacial property between the active and gate dielectric layer. Figure 5 represents TEM cross-sectional images of active bilayer structure IZO:Al/IZO and IZO:Ga/IZO thin films to examine the interface of the thin film layers. The fabricated active bilayer thin films are uniformly coated with a thickness of about 10 nm. The magnified TEM images shown in Figure 5b,d exhibit unclear interfaces between the top and bottom layers representing a very smooth boundary. This smooth interface can enhance the mobility of the heterojunction structure TFTs with a IZO:X bottom layer. Also, the surface roughness of the

Table 2. Chemical Compositions of Active Single-Layer Thin Films Analyzed by XPS

active single-layer	[Al, Ga /(In + Zn)] (%)	In	Zn	O	M−O (%) 530.7 ± 0.1 eV	M−Vo (%) 532.0 ± 0.1 eV	M−OH (%) 532.9 ± 0.1 eV
IZO		11.0	23.2	64.1	72.9	17.3	9.86
IZO:Al (4 mol %)	4.5	21.1	12.4	63.3	68.4	15.4	16.2
IZO:Ga (4 mol %)	3.8	20.2	10.1	67.0	68.3	16.0	15.7

Table 3. Chemical Compositions of Active Bilayer Thin Films Analyzed by XPS

active bilayer (bottom/top)	Ar^+ ion sputtering time (s)	[Al,Ga /(In+Zn)] (%)	In	Zn	O	C	Si
IZO/IZO:Al (4 mol %)	0	0	5.5	9.5	46.6	38.5	0
	20	4.2	9.4	20.6	54.1	0	12.3
	40	5.3	4.7	16.4	53.7	0	21.7
IZO/IZO:Ga (4 mol %)	0	4.4	5.0	7.8	38.0	49.0	0
	20	3.7	8.7	21.9	52.3	0	13.7
	40	4.1	4.0	16.5	54.2	0	22.3
IZO:Al (4 mol %)/IZO	0	0	5.9	9.4	45.0	26.4	0
	20	0	11.3	13.4	58.6	0	13.9
	40	2.6	1.7	2.2	58.4	0	36.0
IZO:Ga (4 mol %)/IZO	0	0	7.0	8.9	40.0	36.0	0
	20	0.78	12.7	14.1	57.5	0	11.6
	40	2.7	2.9	4.8	57.7	0	31.7

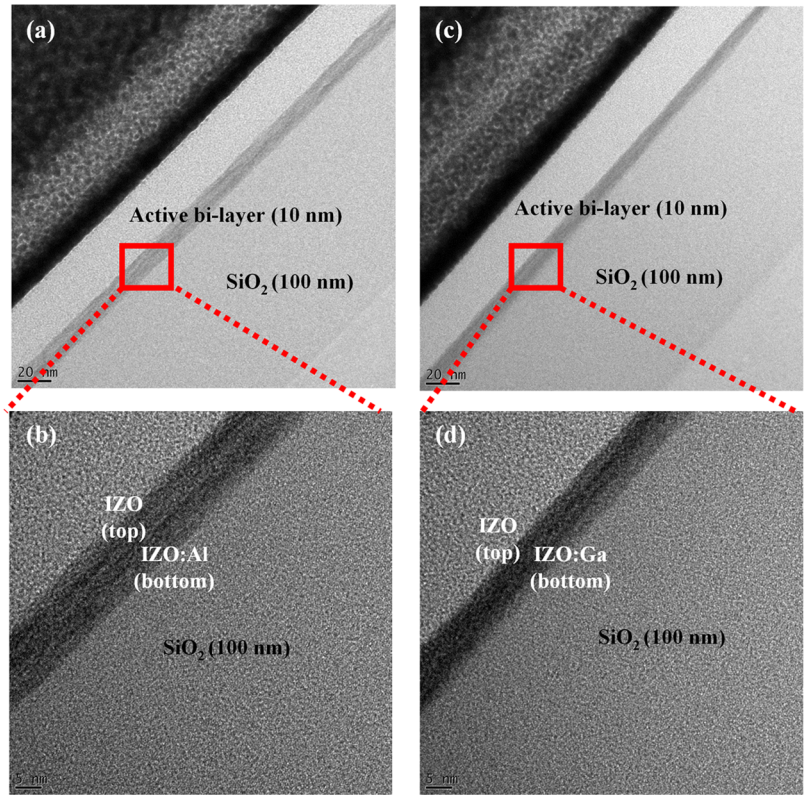

Figure 5. TEM morphology of active bilayer structure TFTs. (a) High resolution cross-sectional image of active bilayer structure IZO:Al/IZO, (b) magnified image of panel a, (c) active bilayer structure IZO:Ga/IZO, and (d) magnified image of panel c.

IZO:Al and IZO:Ga thin films examined by AFM are much smoother (rms roughness is 0.042 and 0.014 nm, respectively) than that of undoped IZO thin film (rms roughness: 0.345 nm) at the nanoscale (see Figure S6, Supporting Information). Thus, all the oxide thin films are uniformly coated with no defects, and the variation of roughness heights is very small. Consequently, the electrical performance in bilayer structure IZO/IZO:X and IZO:X/IZO TFTs are affected by both the oxide/gate dielectric interfacial property of the front-channel layer and the thermal-diffusion of back-channel precursor.[23,27−30]

Generally, a transparent oxide TFT has a wide band gap that includes the various trap sites that deteriorate the stability. The high quality of oxide thin films is controlled by various processes and novel active materials that are very important to good stability with minimum traps and pores.[14,15,36,37] The bias stability in bilayer structure IZO/IZO:X TFTs is influenced by the top-layer IZO:X TFT, which shows improved PBS and degraded NBS resulting from the Al and Ga doping effects. The

bilayer structure IZO/IZO:X TFTs show the best PBS results among all the single- and bilayer structure TFTs. In other bilayer structure IZO:X/IZO TFTs, the bias stability is also influenced by the top-layer IZO TFT, which has the best NBS and the worst PBS properties. Thus, the bilayer structure IZO:X/IZO TFTs show improved NBS and degenerated PBS results in the bias stability compared to the single-layer structure IZO:X TFT. Therefore, both mobility and bias stability in the bilayer structure TFT are influenced by characteristics of top-layer TFT. In particular, the bias stability in the bilayer structure TFTs become better than that of the single-layer structure TFTs because various traps are reduced by thermal diffusion of top-layer composition at high-temperature annealing in the solution process.[27,36]

4. CONCLUSION

The doping of Al and Ga to the aqueous solution processed IZO TFT produces improved positive bias stability, although the mobility is degraded. Thus, the active bilayer structure TFTs with combinations of undoped and doped IZO thin film layers exhibit different levels of the mobility and gate bias stability. These changes are caused by thermal diffusion of the composition in the double coated bilayer thin films. The undoped single-layer IZO TFT shows high mobility with the best NBS result, which is appropriated to AM-LCD back-plane application. On the other hand, the active bilayer structure IZO/IZO:X has the best PBS result, which is suitable for application to AMOLED back-planes. On the basis of these results, the solution-processed TFT performance can be improved with precise control of the composition gradient obtained by a change in the annealing process and in the thickness of the front-channel layer.

■ ASSOCIATED CONTENT

Supporting Information

Associated content, including TGA, XPS analysis, and AFM morphology. This material is available free of charge via the Internet at http://pubs.acs.org.

■ AUTHOR INFORMATION

Corresponding Author

*Byeong-Soo Bae: E-mail: bsbae@kaist.ac.kr.

Notes

The authors declare no competing financial interest.

■ ACKNOWLEDGMENTS

This work was supported by the Materials Original Technology Program (10041222) funded by the Ministry of Knowledge Economy (MKE, Korea).

■ REFERENCES

(1) Nomura, K.; Ohta, H.; Takagi, A.; Kamiya, T.; Hirano, M.; Hosono, H. Room−Temperature Fabrication of Transparent Flexible Thin-Film Transistors Using Amorphous Oxide Semiconductors. *Nature* **2004**, *432*, 488−492.

(2) Hosono, H. Ionic Amorphous Oxide Semiconductors: Material Design, Carrier Transport, and Device Application. *J. Non-Cryst. Solids.* **2006**, *352*, 851−858.

(3) Pasquarelli, R. M.; Ginley, D. S.; O'Hayre, R. Solution Processing of Transparent Conductors: from Flask to Film. *Chem. Soc. Rev.* **2011**, *40*, 5406−5441.

(4) Coneley, J. F. Instabilities in Amorphous Oxide Semiconductor Thin-Film Transistors. *IEEE Trans. Device Mater. Reliab.* **2010**, *10*, 460−475.

(5) Fortunato, E.; Barquinha, P.; Martins, R. Oxide Semiconductor Thin-Film Transistors: A Review of Recent Advances. *Adv. Mater.* **2012**, *34*, 2945−2986.

(6) Hennek, J. W.; Smith, J.; Yan, A.; Kim, M.-G.; Zhao, W.; Dravid, V. P.; Facchetti, A.; Marks, T. J. Oxygen "Getter" Effects on Microstructure and Carrier Transport in Low Temperature Combustion-Processed a-InXZnO (X = Ga, Sc, Y, La) Transistors. *J. Am. Chem. Soc.* **2013**, *135*, 10729−10741.

(7) Han, D.-S.; Moon, D.-Y.; Kang, Y.-J.; Park, J.-H.; Park, J.-W. Improvement in the Negative Bias Stability of Zinc Oxide Thin-Film Transistors by Hafnium Doping. *Curr. Appl. Phys.* **2013**, *13*, S98−S102.

(8) Park, J. C.; Kim, S.; Kim, S.; Kim, C.; Song, I.; Park, Y.; Jung, U.-I.; Kim, D. H.; Lee, J.-S. Highly Stable Transparent Amorphous Oxide Semiconductor Thin-Film Transistors Having Double-Stacked Active Layers. *Adv. Mater.* **2010**, *22*, 5512−5516.

(9) Tue, P. T.; Miyasako, T.; Li, J.; Tu, H. T. C.; Inoue, S.; Tokumitsu, E.; Shimoda, T. High-Performance Solution-Processed ZrInZnO Thin-Film Transistors. *IEEE Trans. Electron Devices* **2013**, *60*, 320−326.

(10) Lim, K.-H.; Kim, K.; Kim, S.; Park, S. Y.; Kim, H.; Kim, Y. S. UV-Visible Spectroscopic Analysis of Electrical Properties in Alkali Metal-Doped Amorphous Zinc Tin Oxide Thin-Film Transistors. *Adv. Mater.* **2013**, *25*, 2994−3000.

(11) Kim, G. H.; Jeong, W. H.; Ahn, B. D.; Shin, H. S.; Kim, H. J.; Kim, H. J.; Ryu, M.-K.; Park, K.-B.; Seon, J.-B.; Lee, S.-Y. Investigation of the Effects of Mg Incorporation into InZnO for High-Performance and High-Stability Solution-Processed Thin Film Transistors. *Appl. Phys. Lett.* **2010**, *96*, 163506.

(12) Jeon, J.-H.; Hwang, Y. H.; Bae, B.-S.; Kwon, H. L.; Kang, H. J. Addition of Aluminium to Solution Processed Conductive Indium Tin Oxide Thin Film for an Oxide thin film Transistor. *Appl. Phys. Lett.* **2010**, *96*, 212109.

(13) Iwasaki, T.; Itagaki, N.; Den, T.; Kumomi, H.; Nomura, K.; Kamiya, T.; Hosono, H. Combinatorial Approach to Thin-Film Transistors Using Multicomponent Semiconductor Channels: An Application to Amorphous Oxide semiconductors in In-Ga-Zn-O system. *Appl. Phys. Lett.* **2007**, *90*, 242114.

(14) Kamiya, T.; Hosono, H. Material Characteristics and Applications of Transparent Amorphous Oxide Semiconductors. *NPG Asia Mater.* **2010**, *2*, 15−22.

(15) Rim, Y. S.; Jeong, W. H.; Kim, D. L.; Lim, H. S.; Kim, K. M.; Kim, H. J. Simultaneous Modification of Pyrolysis and Densification for Low-Temperature Solution-Processed Flexible Oxide Thin-Film Transistors. *J. Mater. Chem.* **2012**, *22*, 12491−12509.

(16) Jeon, J.-H.; Hwang, Y. H.; Jin, J.; Bae, B.-S. Low-Temperature Aqueous Solution Processed Fluorine-Doped Zinc Tin Oxide Thin-Film Transistors. *MRS commun.* **2012**, *2*, 17−22.

(17) Seo, J.-S.; Jeon, J.-H.; Hwang, Y. H.; Park, H.; Ryu, M.; Park, S.-H. K.; Bae, B.-S. Solution-Processed Fluorine-Doped Indium Zinc Oxide Thin-Film Transistors Fabricated on Flexible film at Low Temperature. *Sci. Rep.* **2013**, *3*, 2085.

(18) Jeong, Y.; Bae, C.; Kim, D.; Song, K.; Woo, K.; Shin, H.; Cao, G.; Moon, J. Bias-Stress-Stable Solution-Processed Oxide Thin Film Transistors. *ACS Appl. Mater. Interfaces* **2010**, *2*, 611−615.

(19) Hwang, Y. H.; Bae, B.-S. Effect of Aluminum and Gallium Doping on the Performance of Solution-Processed Indium Oxide Thin-Film Transistors. *J. Display Technol.* **2013**, *9*, 704−709.

(20) Kim, C. H.; Rim, Y. S.; Kim, H. J. Chemical Stability and Electrical Performance of Dual-Active-Layered Zinc-Tin-Oxide/Indium-Gallium-Zinc-Oxide Thin-Film Transistors Using a Solution Process. *ACS Appl. Mater. Interfaces* **2013**, *5*, 6108−6112.

(21) Yu, X.; Zhou, N.; Smith, J.; Lin, H.; Stallings, K.; Yu, J.; Marks, T. J.; Facchetti, A. Synergistic Approach to High-Performance Oxide Thin Film Transistors Using a Bi-layer Channel Architecture. *ACS Appl. Mater. Interfaces* **2013**, *5*, 7983−7988.

(22) Kim, S. I.; Park, J.-S.; Kim, C. J.; Park, J. C.; Song, I.; Park, Y. S. High Reliable and Manufacturable Gallium Indium Zinc Oxide Thin-Film Transistors Using the Double Layers as an Active layer. *J. Electrochem. Soc.* **2009**, *156*, H184−H187.
(23) Park, J. C.; Lee, H.-Y. Improvement of the Performance and Stability of Oxide Semiconductor Thin-Film Transistors Using Double-Stacked Active Layers. *IEEE Electron Device Lett.* **2012**, *33*, 818−820.
(24) Wang, S.-L.; Yu, J.-W.; Yeh, P.-C.; Kuo, H.-W.; Peng, L.-H.; Fedyanin, A. A.; Mishina, E. D.; Sigov, A. S. High Mobility Thin Film Transistors with Indium Oxide/Gallium oxide Bi-Layer Structures. *Appl. Phys. Lett.* **2012**, *100*, 063506.
(25) Kim, S. I.; Kim, C. J.; Park, J. C.; Song, I.; Kim, S. W.; Yin, H.; Lee, E.; Lee, J. C.; Park, Y. High Performance Oxide Thin Film Transistors with Double Active Layers. *IEDM Technol. Dig.* **2008**, 73−76.
(26) Hsu, H.-H.; Chang, C.-Y.; Cheng, C.-H.; Chiou, S.-H.; Huang, C.-H. High Mobility Bilayer Metal-Oxide Thin Film Transistors Using Titanium-Doped InGaZnO. *IEEE Electron Device Lett.* **2014**, *35*, 87−89.
(27) Jung, H. Y.; Kang, Y.; Hwang, A. Y.; Lee, C. K.; Han, S.; Kim, D.-H.; Bae, J.-U.; Shin, W.-S.; Jeong, J. K. Origin of the Improved Mobility and Photo-Bias Stability in a Double-Channel Metal Oxide Transistor. *Sci. Rep.* **2014**, *4*, 3765.
(28) Ahn, C. H.; Kim, S. H.; Cho, S. W.; Yun, M. G.; Cho, H. K. Double-Layer Channel Structure based ZnO Thin-Film Transistor Grown by Atomic layer Deposition. *Phys. Status Solidi RRL* **2014**, *8*, 328−331.
(29) Ahn, C. H.; Yun, M. G.; Lee, S. Y.; Cho, H. K. Enhancement of Electrical Stability in Oxide Thin-Film Transistors Using Multilayer Channels Grown by Atomic Layer Deposition. *IEEE Trans. Electron Devices* **2014**, *61*, 73−78.
(30) Nag, M.; Chasin, A.; Rockele, M.; Steudel, S.; Myny, K.; Bhoolokam, A.; Tripathi, A.; Putten, B.; Kumar, A.; Steen, J.-L.; Genoe, J.; Li, F.; Maas, J.; Veenendaal, E.; Gelinck, G.; Heremans, P. Single-Source Dual-Layer Amorphous IGZO Thin-Film Transistors for Display and Circuit Applications. *J. Soc. Inf. Disp.* **2013**, *21*, 129−136.
(31) Tian, Y.; Han, D.; Zhang, S.; Huang, F.; Shan, D.; Cong, Y.; Cai, J.; Wang, L.; Zhang, S.; Zhang, X.; Wang, Y. High-Performance Dual-Layer Channel Indium Gallium Zinc Oxide Thin-Film Transistors Fabricated in Different Oxygen Contents at Low Temperature. *Jpn. J. Appl. Phys.* **2014**, *53*, 04EF07.
(32) Rudolph, W. W.; Pye, C. C.; Irmer, G. Study of Gallium(III) Nitrate Hydrate and Aqueous Solutions: Raman Spectroscopy and *ab initio* Molecular Orbital Calculations of gallium(III) Water Clusters. *J. Raman Spectrosc.* **2002**, *33*, 177−190.
(33) Ionic Potential. http://en.wikipedia.org/wiki/Ionic_potential (accessed Oct, 2014), Wikipedia.
(34) Lide, D. R. *Handbook of Chemistry and Physics*, 75th ed; CRC Press: Boca Raton, FL, 1994.
(35) Liu, L.-C.; Chen, J.-S.; Jeng, J.-S. Role of Oxygen Vacancies on the Bias Illumination Stress Stability of Solution-Processed Zinc Tin Oxide Thin Film Transistors. *Appl. Phys. Lett.* **2014**, *105*, 023509.
(36) Kim, S. J.; Yoon, S.; Kim, H. J. Review of Solution-Processed Oxide Thin-Film Transistors. *Jpn. J. Appl. Phys.* **2014**, *53*, 02BA02.
(37) Martins, R.; Barquinha, P.; Ferreira, I.; Pereira, L.; Gonçcalves, G.; Fortunato, E. Role of Order and Disorder on the Electronic Performances of Oxide Semiconductor Thin Film Transistors. *J. Appl. Phys.* **2007**, *101*, 044505.